Nanostructured germanium prepared via ion beam modification

Nicholas Guy Rudawski[a)]
Major Analytical Instrumentation Center, University of Florida, Gainesville, Florida 32611
Kevin Scott Jones
Department of Materials Science and Engineering, University of Florida, Gainesville, Florida 32611

(Received 26 November 2012; accepted 31 January 2013)

"Nanostructured" germanium (Ge; also known as "voided," "porous," "nanoporous," "cratered," and "honeycomb" Ge) created via ion beam modification has been studied for many years. This work reviews the progress made in studying and characterizing the nanostructured morphology, particularly via the use of experimental techniques such as scanning electron microscopy, atomic force microscopy, and transmission electron microscopy. Specifically, the empirical observations of the structural evolution of Ge as a function of ion beam modification conditions are discussed with added emphasis placed on quantification of the microstructure. The experimental observations and microstructure quantification are further discussed in terms of the implications for proposed formation mechanisms of the nanostructured morphology. Potential uses of the nanostructured morphology in chemical sensor and energy storage applications and suggested future lines of research to further the fundamental understanding of nanostructuring in Ge using ion beam modification are also presented.

I. INTRODUCTION

So-called "nanostructured" materials,[1] which have characteristic feature sizes of the order of a few to tens of nm, are attractive in a wide range of applications including energy storage,[2–5] thermoelectrics,[6] photovoltaics,[7] chemical sensors,[8–10] photodetectors,[11] drug delivery,[12] and structural applications[13] and can be produced via a variety of methods including chemical/physical vapor deposition,[1] micromachining,[12] and electrochemical cycling.[14] One of the more interesting methods of nanostructuring is via the use of ion beam modification (interchangeably referred to as ion-implantation). In particular, for the case of a few different types of semiconducting materials, ion beam modification under appropriate conditions is known to result in complete structural decomposition of a material with no or very little initial porosity to a porous microstructure consisting of a nanoscale interdigitated network of strands. This process is known to occur for several different semiconductors, and was first demonstrated for the case of compound semiconductors such as indium antimonide (InSb), gallium antimonide (GaSb), and gallium nitride (GaN).[15–19] However, It was not until the early 1980s that it was discovered that the elemental semiconductor Ge also experiences a similar phenomenon,[20–23] which has to date been most extensively studied as compared with any other materials that exhibit similar behavior. Nanostructuring of Ge using ion beam modification will be the subject of this review, but it should be noted that many, if not all, considerations discussed here in the context of Ge may not be applicable to the aforementioned materials that exhibit similar phenomena.

The basic process of structural decomposition of Ge using ion beam modification is described as follows: starting with a single-crystal Ge substrate, if the material is ion-beam modified with relatively heavy ions up to a critical dose, an amorphous (α) layer will form in the material, the extent of which depends mainly on the energy of the incident ions; if the dose is further increased beyond this amorphization threshold, the material will begin to structurally decompose and exhibit macroscopic voiding and porosity; with further increasing dose, the material eventually transforms into the aforementioned morphology consisting of a nanoscale interdigitated network of strands. Figure 1 presents top-down scanning electron microscopy (SEM) and cross-sectional transmission electron microscopy (XTEM) images showing an initially single-crystal Ge specimen that was rendered into the nanostructured morphology by Ge^+-implantation at 260 keV at room temperature to a dose of 1.0×10^{16} cm^{-2}. This morphology as been variously referred to by many different labels over several decades of study as "voided," "porous," "nanoporous," "cratered," and "honeycomb," but for the purpose of this study, this morphology will be referred to as "nanostructured" as first termed by Romano et al.[24]

As previously mentioned, the structural decomposition of Ge due to ion beam modification has been extensively studied and characterized by several independent research groups over several decades. The process is known to be most sensitive to ion dose,[21,24–28] specimen temperature during implantation,[20,27,29,30] and, most interestingly, the

[a)]Address all correspondence to this author.
e-mail: ngr@ufl.edu
DOI: 10.1557/jmr.2013.24

 © Materials Research Society 2013

https://doi.org/10.1557/jmr.2013.24 Published online by Cambridge University Press

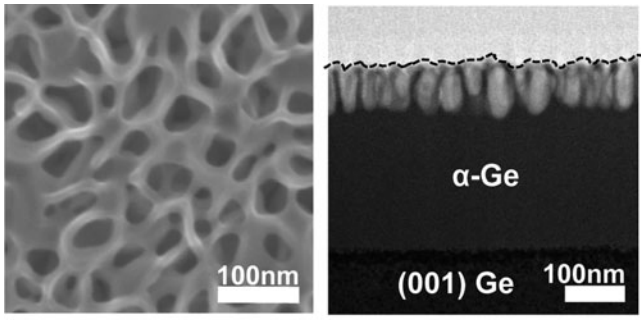


FIG. 1. Images of nanostructured Ge formed by Ge^+-implantation at 260 keV at room temperature to a dose of 1.0×10^{16} cm^{-2} into single-crystal (001) Ge: (a) top-down SEM and (b) XTEM (surface indicated by dotted line).

nature of the starting material prior to ion beam modification (amorphous versus crystalline).[28,31] However, while the structural decomposition of Ge has been studied and characterized empirically quite extensively, the fundamental understanding of nanostructuring due to ion beam modification remains a topic of debate. To date, two fundamentally different models have been advanced to explain the origin of structural decomposition due to ion beam modification: vacancy clustering and "microexplosions." The vacancy-clustering model[22,24,30,32–34] is based on the premise of inefficient recombination of point defects in the material (which is known to be the case for Ge[35]) generated due to ion beam modification, which results in an excess quantity of vacancies that coalesce to form macroscopic voids. In contrast, the microexplosion model[36–39] is based on the creation of voids through pressure waves and thermal spikes due to the overlap of ion cascades during ion beam modification. In the light of the rather large base of empirical work regarding nanostructuring of Ge due to ion beam modification, it is somewhat surprising that a more concerted effort has not yet been made to discuss the implications of the observed experimental results in terms of the proposed formation mechanisms.

This work therefore reviews the current understanding of nanostructuring in Ge due to ion beam modification. Specifically, the empirical observations associated with the process will be discussed as well as the efforts to characterize and quantify the microstructure. A special effort will be placed on discussing the implications of the empirical observations in terms of the two proposed formation mechanisms to provide insight into the fundamental nature of nanostructuring in Ge due to ion beam modification.

II. BASIC OBSERVATIONS AND MICROSTRUCTURAL EVOLUTION

It has been well established that Ge undergoes a crystalline to amorphous phase transformation as a result of ion beam modification.[40–43] This amorphization process is accepted to be the result of an accumulation of a critical concentration of point defects resulting from ion beam modification such that the material experiences a first-order crystalline to amorphous phase transformation. In the case of single-crystal Ge with a free surface ion beam-modified at room temperature with relatively heavy ions (Ge^+, e.g.,) amorphization is known to occur for ion doses greater than 5.0×10^{13} cm^{-2}.[40–44] If the ion dose is further increased, the material will remain amorphous up to a dose of $\sim 2.0 \times 10^{15}$ cm^{-2}, but if the dose is increased just beyond this, the material will start to structurally decompose and exhibit "pore clusters," which nucleate at the free surface of the material.[25] It is important to note that the crystalline to amorphous transition appears to be necessary prior to the occurrence of nanostructuring; in other words, the material must first exhibit a bulk amorphous structure prior to any pore nucleation, though it is not understood why this is the case. If the dose is further increased, the pores (also interchangeably referred to as "voids" or "craters") completely cover and rupture the surface while becoming larger and somewhat elongated along the direction of the incident ions, generating a layer with the nanostructured morphology on top of a nonporous α-Ge layer.[21,24–28] As the dose further increases, the nanostructured layer experiences a large out-of-plane expansion with the individual pores continuing to elongate and the surface experiencing increased roughening;[24,25] an underlying α-Ge layer remains under the nanostructured layer, but while the thickness of the nanostructured layer continues to increase with increasing dose, the thickness of the underlying α-Ge layer remains relatively constant. This complete morphological evolution of Ge with increasing ion dose is presented schematically in Fig. 2.

Likewise, Figs. 3(a)–3(c) present XTEM images of nanostructured Ge prepared by Ge^+-implantation at 130 keV at room temperature to doses of 1.0×10^{16}, 3.0×10^{16}, and 1.0×10^{17} cm^{-2}. The evolution of the pore size and morphology as well as the thickness of the nanostructured layer with increasing ion dose is clearly evident as described previously. Additionally, a "damage map" adapted from Darby et al.[25] displays the relationship between incident ion energy, dose, and resulting microstructure for Ge^+-implantation at room temperature into single-crystal Ge as presented in Fig. 4; it is evident that ion dose is the primary factor that controls morphological evolution. In addition to this qualitative observation of the morphological evolution, work regarding the quantification of the nanostructured morphology as a function of ion beam modification conditions has also been performed as will be discussed in detail in a subsequent section.

The dose-dependence of the morphological evolution is the most well known aspect of nanostructuring in Ge due to ion beam modification. However, the process is also known to be sensitive to the substrate temperature[20,27,29,30,45] maintained during ion beam modification as well as the nature of

https://doi.org/10.1557/jmr.2013.24 Published online by Cambridge University Press

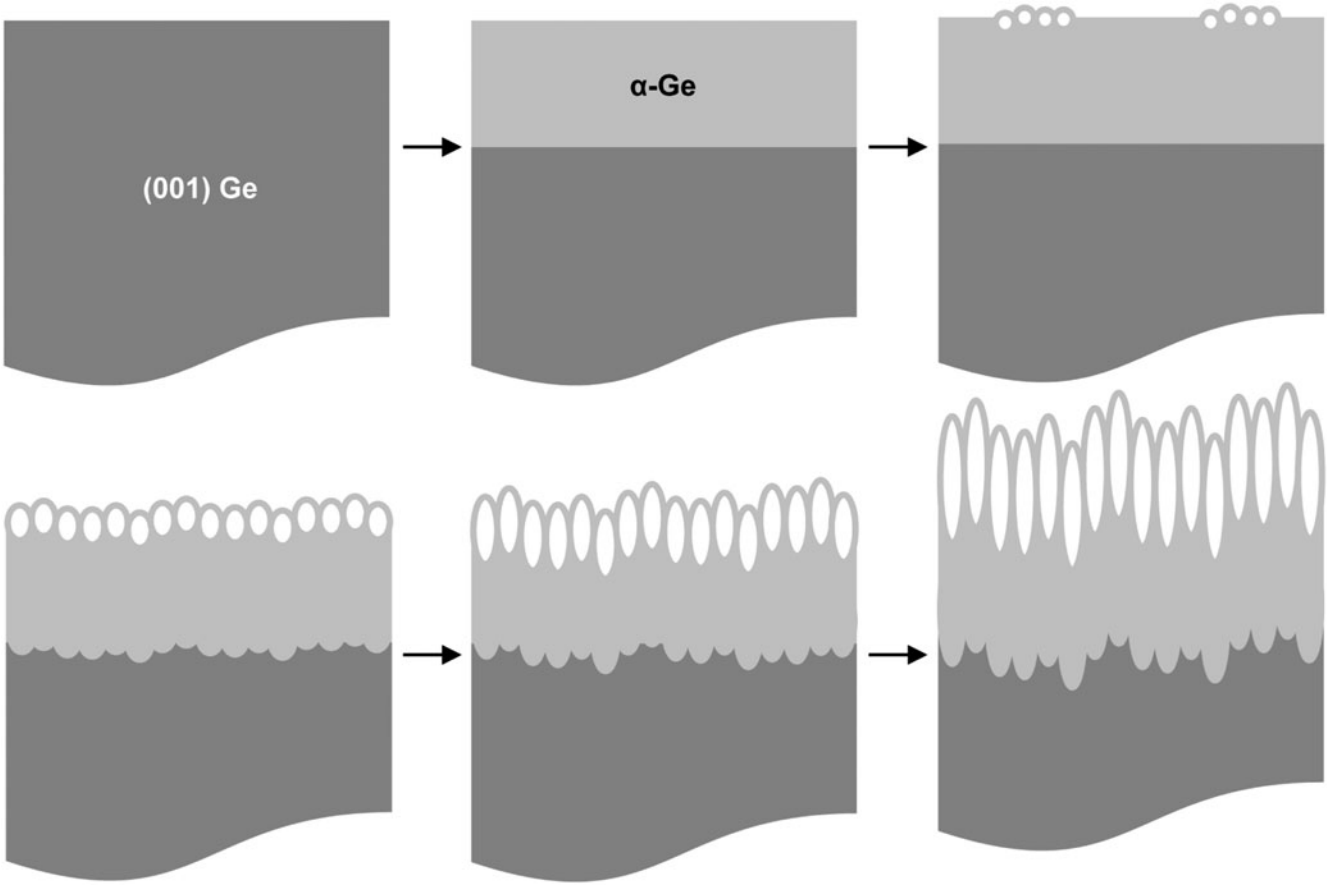


FIG. 2. Schematic representation of the microstructural evolution of Ge with increasing ion dose; the starting material is single crystal Ge, but with increasing dose an amorphous layer is formed; as the dose increases further, small clusters of near-surface pores nucleate; as the dose increases further, the pores cover the whole surface and elongate into the wafer, forming the nanostructured morphology; as the dose increases further, the pores elongate further and the material experiences a large out-of-plane expansion with the nanostructured region existing on top of a nonporous amorphous layer. In all cases, the surface roughness and roughness of the amorphous/crystalline interface increase with increasing ion dose.

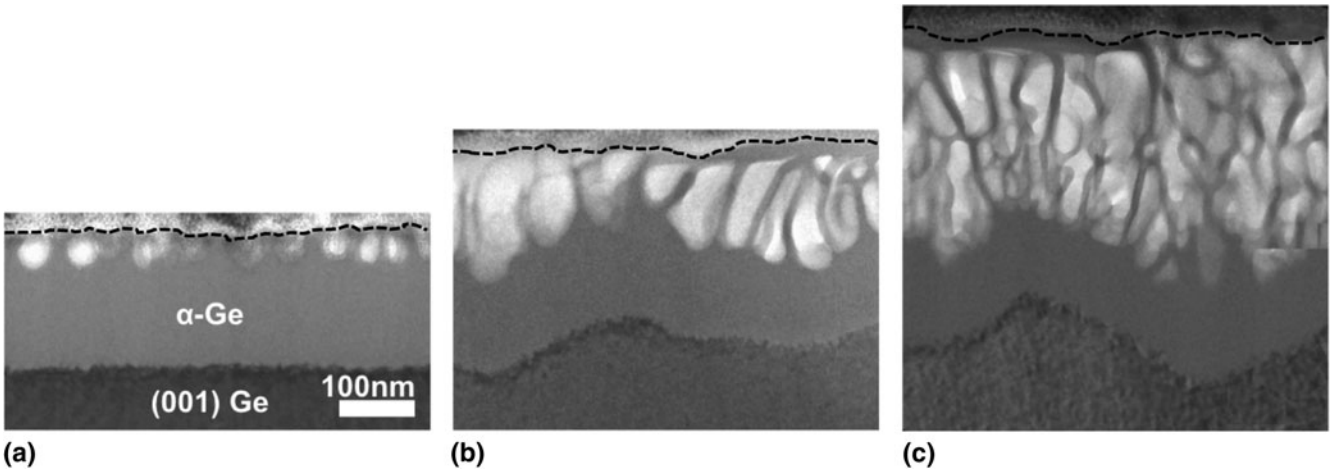


FIG. 3. XTEM images showing the morphological evolution of nanostructuring in Ge with increasing ion dose as a result of Ge^{+}-implantation at 130 keV at room temperature into single-crystal (001) Ge: (a) 1.0×10^{16}, (b) 3.0×10^{16}, and (c) 1.0×10^{17} cm^{-2} ion doses. Reproduced and modified with permission from Darby et al.[25] Copyright © 2011 by Elsevier. Reprinted by permission of Elsevier.

the material prior to ion beam modification;[28,31,46] both of these factors will be discussed in detail in subsequent sections of this review. These basic considerations noted, finer details regarding quantification of the nanostructured morphology, the role of temperature during implantation, the influence of the starting material microstructure, and

https://doi.org/10.1557/jmr.2013.24 Published online by Cambridge University Press

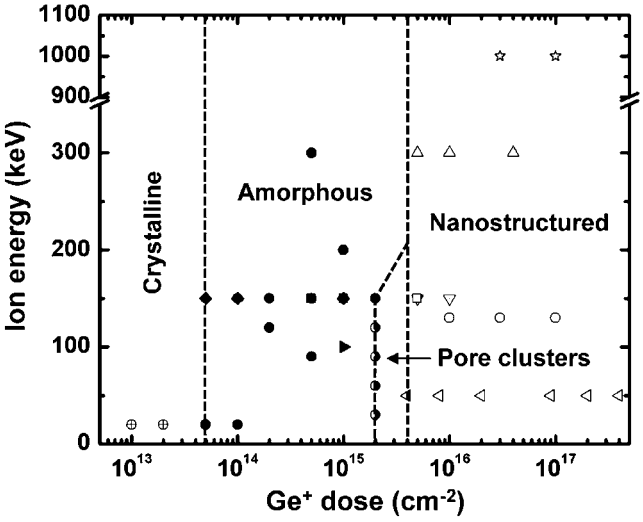


FIG. 4. Implant "damage map" showing the resultant microstructure of Ge as a function of Ge^+ ion energy and dose at room temperature (initially single crystal material); the sources for each reported data point are specified elsewhere.[25] Reproduced and modified with permission from Darby et al.[25] Copyright © 2011 by Elsevier. Reprinted by permission of Elsevier.

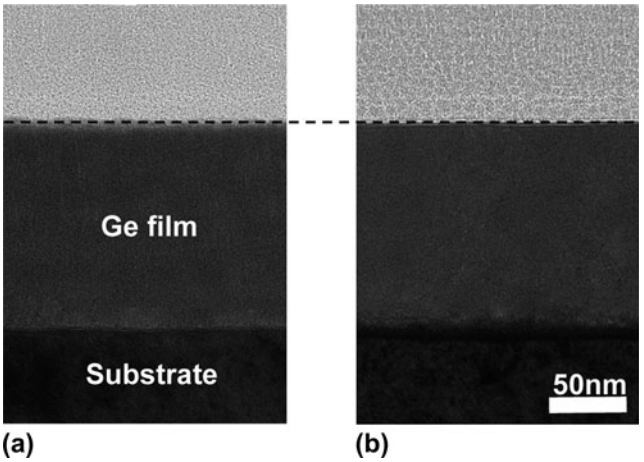


FIG. 5. XTEM images of an as-deposited amorphous Ge film on a metallic substrate: (a) as-deposited and (b) after Ge^+-implantation at 260 keV to a dose of 1.0×10^{16} cm^{-2} at $T = -196$ °C showing that nanostructuring can be suppressed when ion beam modification is performed outside the so-called "temperature window" (surface indicated by dotted line). Reproduced and modified with permission from Rudawski et al.[45] Copyright © 2013 by Elsevier. Reprinted by permission of Elsevier.

the implications of the empirical observations for the proposed formation mechanisms will be presented.

III. "TEMPERATURE WINDOW" FOR NANOSTRUCTURING

As stated previously, the temperature at which ion beam modification is performed has a profound influence on the nanostructuring process. It was first revealed by Appleton et al.[20] using XTEM that by performing ion beam modification at temperature $T = -196$ °C it was possible to suppress nanostructuring in initially single-crystal Ge. Shortly after, work by Holland et al.[22] confirmed this observation, but also produced the interesting result that nanostructuring was suppressed when $T > 300$ °C. More than two decades later, work by Ottaviano et al.[34] also investigated the role of specimen temperature during ion beam modification on resulting morphology using top-down SEM, but revealed that nanostructuring was suppressed when $T > 240$ °C, which is a discrepancy of ~60 °C as compared with the result of Holland et al.[22] To date, the most complete study on the temperature influence on nanostructuring in Ge due to ion beam modification can be credited to Strizker et al.[27] who used XTEM to investigate the resulting material morphology as a function of temperature during ion beam modification for a wide temperature range over relatively fine temperature increments and determined that a "temperature window" for nanostructuring existed for—$80 \leq T \leq 200$ °C. Additionally, recent work by Rudawski et al.[45] revealed that nanostructuring was suppressed for ion beam modification at $T = -196$ °C into an as-deposited amorphous Ge film as shown in Fig. 5, so the effect appears to be somewhat independent of starting material structure. It is also noteworthy that when the temperature is above the upper range of temperature window, the material never experiences amorphization or nanostructuring during ion beam modification[22]; this is consistent with the findings presented in Fig. 4 showing that it is necessary for the material to be become amorphous during ion beam modification (or be amorphous prior to ion beam modification) for nanostructuring to occur.

It is evident that among the work that investigated the upper range of the temperature window for nanostructuring there appears to be some discrepancies in the upper limit to suppress nanostructuring.[22,27,34] Perhaps a difference in the energy regimes used for ion beam modification in each study may have been a causal factor, as the work of Holland et al.[22] and Ottaviano et al.[34] used ion energies of the order of hundreds of keV while the work of Strizker et al.[27] used energies of 1 MeV. Yet, considering the similar nature of the former two studies, it is still somewhat unclear why there would be a discrepancy to the extent of 60 °C for the upper temperature limit for nanostructuring. In any case, the presence of a temperature window for nanostructuring due to ion beam modification indicates that competing thermally activated process may play a role in the fundamental formation mechanism; this temperature window will be revisited subsequently when the implications of experimental observations for proposed mechanisms are discussed.

https://doi.org/10.1557/jmr.2013.24 Published online by Cambridge University Press

IV. MORPHOLOGICAL QUANTIFICATION

Whereas structural decomposition of Ge due to ion beam modification has been studied for several decades, relatively little work has focused on quantification of the nanostructured morphology with most studies having been predisposed towards qualitative observations. In this section, the many attempts to quantify the nanostructured morphology are reviewed. Using the treatment of Romano et al.,[24] the features of the nanostructured morphology that are discussed are the pore radius (R) distribution and areal pore density (Q) as viewed in top-down orientation, the thickness of the nanostructured layer (h) when viewed in cross-sectional orientation, the out-of-plane swelling (s) as measured relative to the position of the virgin surface prior to ion beam modification, and surface roughness.

The first attempt at quantification of the changes in microstructure in Ge due to ion beam modification should probably be credited to Wilson et al.,[21] who used top-down SEM to investigate the average pore radius (R_{avg}) as a function of ion dose (Φ) for a given ion energy and revealed that R_{avg} increases with increasing dose until somewhat of a saturation point is reached. Later work by Ottaviano et al.[34] and Romano et al.[24,28] also used top-down SEM to quantify the R distribution. The results from Romano et al.[24,28] largely confirm what Wilson et al.[21] first quantified roughly three decades earlier; some of these findings are presented in Figs. 6(a)–6(c), which present top-down SEM images of nanostructured Ge prepared by Ge^+-implantation at 300 keV at room temperature to doses of 5.0×10^{15}, 1.0×10^{16}, and 4.0×10^{16} cm^{-2}, respectively. Figure 7 shows the quantified R distributions for each of these doses and confirms that R_{avg} increases with dose. The work of Ottaviano et al.[34] also produced the interesting result that R tended to decrease with increasing substrate temperature during ion beam modification and nanostructuring. In both cases, an inverse relationship between R_{avg} and Q was demonstrated and is evident from Fig. 5.[24,28,34] Additionally, Romano et al. quantified Q as a function of ion dose for Ge^+-implantation at 300 keV at room temperature into single-crystal Ge for ion doses $\geq 5.0 \times 10^{15}$ cm^{-2} and confirmed this relationship as presented in Fig. 8. However, Darby et al.[25] used plan-view TEM and measured $R_{avg} = 8 \pm 3$ nm and $Q = 4.0 \times 10^9$ for Ge^+-implantation at 90 keV at room temperature to a dose of 2.0×10^{15} cm^{-2}. Whereas the value of ion energy is not the same as that used by Romano et al.,[24] it is interesting that this value for R_{avg} is consistent with the trend observed in Fig. 7 in that R_{avg} tends to increase with ion dose. However, the value of Q is not consistent with that reported in Fig. 7 in that it is actually smaller for a lower dose. Thus, if the Q versus ion dose data were collected for a larger dose range, it may actually obey the trend indicated by the continuous line superimposed on Fig. 8 where a maximum in the curve may be observable at some particular dose.

Of course, as stated earlier, the pores tend to evolve in an elongated fashion as the ion dose is increased (at least when the starting material is single crystal), which results in an increase in h with increasing dose; this increase in h with ion dose is related to the macroscopic out-of-plane swelling, s, but is not exactly the same as will be discussed shortly. Romano et al.[24] were the first to quantify h using several different cross-sectional approaches including cross-sectional SEM and XTEM. Using an argument that the total volume of the pores was equivalent to the total amount of excess vacancies, it was ultimately revealed that h obeyed the following relationship:

$$\pi Q R_{avg}^2 h = \frac{n_{vac}}{\rho_{Ge}} (\Phi - \Phi_0) \quad , \tag{1}$$

where n_{vac} is the number of vacancies created per incident ion as predicted by simulations,[47] ρ_{Ge} is the density of

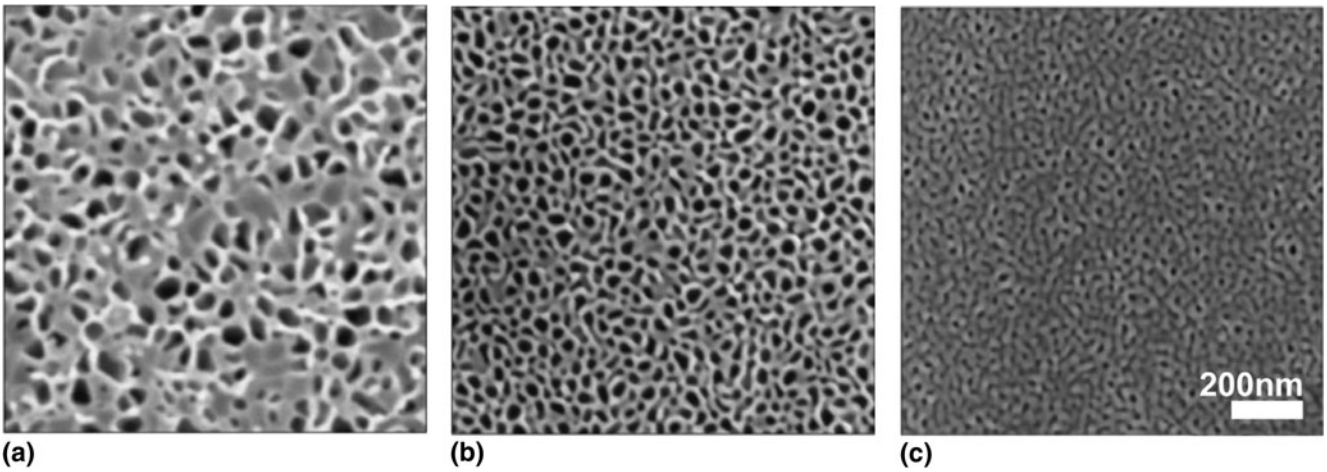


FIG. 6. Top-down SEM images of nanostructured Ge prepared by Ge^+-implantation at 300 keV into (001) Ge to doses of (a) 5.0×10^{15}, (b) 1.0×10^{16}, and (c) 4.0×10^{16} cm^{-2}. Reproduced and modified with permission from Romano et al.[24] Copyright © 2010 by the American Institute of Physics. Reprinted by permission of the American Institute of Physics.

https://doi.org/10.1557/jmr.2013.24 Published online by Cambridge University Press

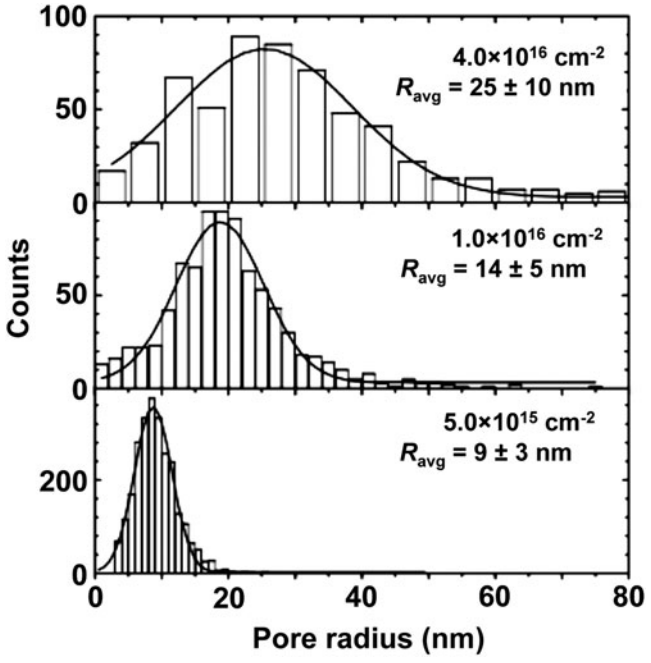


FIG. 7. Pore radius distribution of nanostructured Ge prepared by Ge^+-implantation at 300 keV into single-crystal (001) Ge for doses of 5.0×10^{15}, 1.0×10^{16}, and 4.0×10^{16} cm^{-2} as measured by top-down SEM; the average pore radius (R_{avg}) for each dose is indicated. Reproduced and modified with permission from Romano et al.[24] Copyright © 2010 by the American Institute of Physics. Reprinted by permission of the American Institute of Physics.

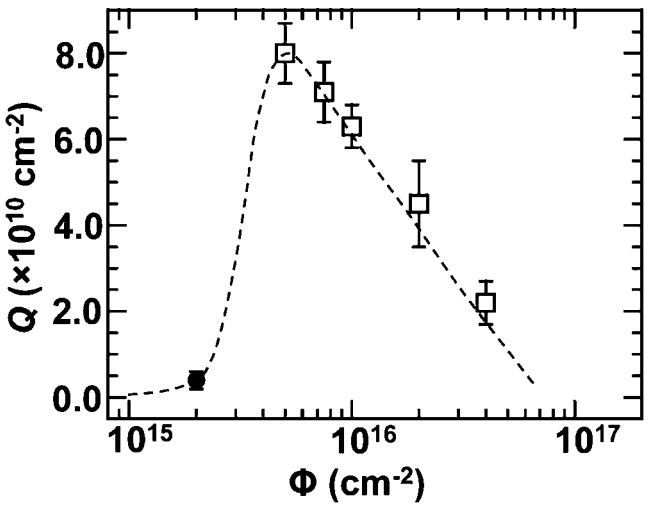


FIG. 8. Areal pore density as a function of ion dose for nanostructured Ge prepared by Ge^+-implantation at room temperature into single-crystal Ge as reported by Romano et al.[24] for an ion energy of 300 keV (□) and Darby et al.[25] for an ion energy of 90 keV (□); the dotted line indicates the general trend of the data and does not correspond to the fit of any model.

Ge, Φ is the ion dose, and Φ_0 is the threshold dose for nanostructuring; the total volume of the pores per unit surface area is thus $\pi Q R_{avg}^2 h$ and is expected to increase linearly with dose, which was consistent with observations.[24]

Of course, it should be noted that h and s, while clearly related, are actually different as h is the thickness of the nanostructured layer whereas s is the swelling relative to the virgin surface position; in fact, it was not until relatively recently that the difference between h and s was actually delineated through careful measurement.[24] Prior to this, researchers were quantifying the change in surface position relative to the virgin surface location, which of course is s, though it was thought at times that the amount of swelling was indicative of the total thickness of material that had been rendered nanostructured, which is h. Huber et al.[33] first quantified s a function of ion dose for different incident ion energies in the range of a few hundred MeV using atomic force microscopy (AFM). It was determined that s could be modeled after Prins et al.[48] as

$$s = s_{\max}\left[1 - e^{-(a\Phi+b)}\right] \quad , \qquad (2)$$

where s_{max} is the maximum out-of-plane swelling, a is a constant with units of cm^2 i.e., related to the number of vacancies produced per incident ion, and b is pure fitting constant. The parameters s_{max}, a, and b all depend on the incident ion mass and energy; specifically, it was shown that all three increase with increasing ion energy.[33] Work by Strizker et al.[27] also quantified s as function of ion dose at ion energies of the order of a few MeV using XTEM and produced results that qualitatively agreed with those of Huber et al.[33] but tended to show a linear relationship between s and ion dose. Work several years later by Steinbach et al.[49] also produced similar results showing a linear relationship between s and ion dose, but at ion energies of the order of a few hundred MeV, which again contradicts the findings of Huber et al.[33]

More recently, Romano et al.[24] also quantified s using AFM, but at ion energies of the order of a few hundred keV. In similarity to the results from the three previously studies, an increase in s with ion dose was revealed. However, the s-ion dose relationship did not appear to obey the relationship advanced by Huber et al.[33] using Eq. (2) or the linear relationship of Strizker et al.[27] and Steinbach et al.[49] Rather, s tended to increase exponentially with ion dose. The difference between the results of Romano et al.[24] and the other three studies may be due to the ion energies used in each study. Specifically, the former used ion energies of the order of a few hundred keV whereas the later used ion energies of the order of a few to a few hundred MeV; therefore the ion energy regime may play a role in the evolution of s with ion dose. Although, the issue of why some have shown a swelling-ion dose relationship for the ion energy regime of a few to a few hundred MeV consistent with Eq. (2) and others have shown a linear relationship for the same energy regime remains unclear. More importantly, Romano et al.[24] were able to delineate the difference between h and s via the use of

https://doi.org/10.1557/jmr.2013.24 Published online by Cambridge University Press

both AFM and XTEM. Specifically, it was shown that the following relationships govern the relationship between h, s, and the projected range of the ions (R_p):

$$h = s \left(s \leq R_p\right) \quad , \tag{3}$$

and

$$h = s + R_p \left(s > R_p\right) \quad . \tag{4}$$

Thus, the nanostructured layer thickness is never smaller than the out-of-plane swelling, but when the amount of swelling is much larger than R_p (e.g., when the ion energy is relatively low) h is nearly equal to s. Figures 9(a)–9(c) present XTEM images of nanostructured Ge prepared by Ge^+-implantation at 300 keV to doses of 1.0×10^{16}, 2.0×10^{16}, and 4.0×10^{16} cm^{-2}; the evolution of h and s as predicted by Eq. (3) is clearly evident.

As evidenced in Fig. 3, it is clear that there tends to be surface roughening resulting from ion beam modification-induced structural decomposition. Several studies have shown that the surface roughness does increase as a result of ion beam modification-induced nanostructuring;[24,34,50–52] however, relatively few studies have characterized this surface roughening as a function of ion beam modification conditions. Chen et al.[32] were the first to quantify surface roughening as a result of ion beam modification-induced nanostructuring using AFM and revealed that the surface roughness increased approximately linearly with ion dose whereas the surface roughness tended to increase with decreasing ion energy for a given ion dose; additional work also investigated the role of beam current density during ion beam modification on surface roughness, but did not indicate a very large effect. Later work by Kaiser et al.[26] also quantified the surface roughening associated with formation of the nanostructured morphology as a function of ion dose for several different ion masses and ion energies using AFM. In general, it was shown that the surface roughness tended to increase with increasing dose for a given ion mass and energy; however, the roughness tended to increase with ion energy for a given ion dose, which is somewhat contradictory in relation to the earlier results of Chen et al.[32] More interestingly, the same work by Kaiser et al.[26] revealed that there is also some dependence of surface roughness on dose rate, with roughness observed to increase with dose rate for a given ion dose and energy, which again somewhat contradicts Chen et al.[32] The discrepancy between Chen et al.[32] and Kaiser et al.[26] may once again be due to the range of ion energies used in each study as the former investigated ion energies of the order of tens of keV whereas the later investigated energies of the order of a few hundred keV; presumably the dose rate effect then only becomes noticeable at high ion energies.

Summarizing the prior work on quantifying the nanostructured morphology, the main considerations have focused on the pore radius distribution, the thickness of

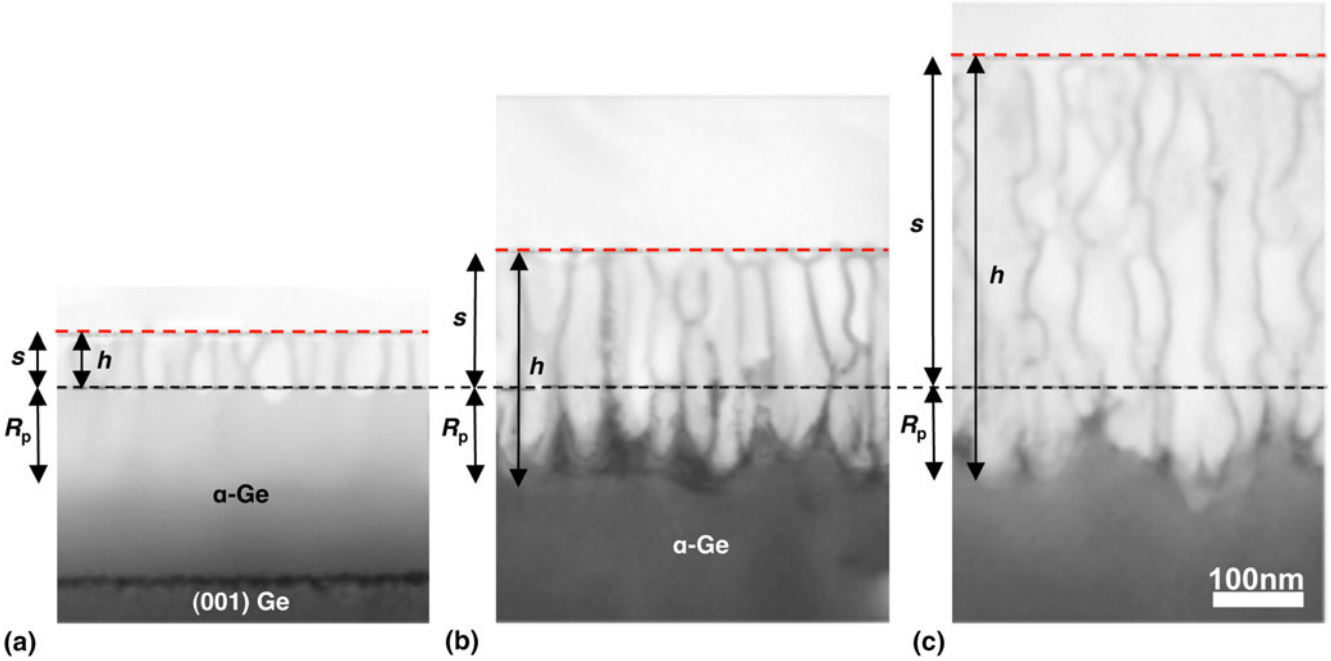


FIG. 9. XTEM images showing the out-of-plane swelling (s) and nanostructured layer height (h) for Ge^+-implantation at 300 keV to doses of: (a) 1.0×10^{16}, (b) 2.0×10^{16}, and (c) 4.0×10^{16} cm^{-2}. The black dotted line indicates the initial position of the specimen surface prior to ion beam modification whereas the red line indicates the actual specimen surface; the projected range (R_p) of the incident ions relative to the initial surface position is also indicated. Reproduced and modified with permission from Romano et al.[24] Copyright © 2010 by the American Institute of Physics. Reprinted by permission of the American Institute of Physics.

https://doi.org/10.1557/jmr.2013.24 Published online by Cambridge University Press

the nanostructured layer, the out-of-plane swelling, and the surface roughness. These efforts are noteworthy, not only because of the importance for potential applications of the nanostructured morphology, but also for the implications for the proposed formation mechanisms as will be revisited later.

V. INFLUENCE OF STARTING MATERIAL

The vast majority of reported work studying the macroscopic considerations of nanostructuring of Ge via ion beam modification utilized single crystals for the initial material. However, as first shown by Peto et al.[53] it has been demonstrated that the starting material does not need to be crystalline for nanostructuring to occur. Specifically, nanostructuring has been demonstrated to occur in amorphous Ge films prepared via electron beam evaporation,[46] as well as sputter deposition,[28,31,53] and molecular beam epitaxy (MBE),[54] and also in starting material that was initially polycrystalline.[54] In the case of material that was initially polycrystalline, the material exhibited a transition to a bulk amorphous morphology prior to nanostructuring, in similarity to the case of initially single-crystal material.[54] Figure 10 presents XTEM images showing as-deposited amorphous Ge becoming nanostructured as a result of Ge^+-implantation at 260 keV at room temperature to a dose of 1.0×10^{16} cm^{-2}. More curiously, it has been demonstrated that the nature of the starting material plays a role in the final morphology of the material following ion beam modification.

Romano et al.[28] were the first to show qualitatively and quantitatively the differences between nanostructured Ge formed via ion beam modification with initial single-crystal or as-deposited amorphous starting material. Specifically, it was shown that the as-deposited amorphous material did not exhibit the elongated pore structure that was observed in the case of single-crystal starting material. Additionally, the thickness of the material that was rendered nanostructured was approximately twice as great for the case of the as-deposited amorphous Ge material as compared with the single-crystal material; Figs. 11(a) and 11(b) present top-down SEM images of nanostructured Ge prepared from single-crystal (001) and amorphous Ge deposited via MBE by Ge^+-implantation at 300 keV at room temperature to a dose of 1.0×10^{16} cm^{-2}; it is evident that the average pore radius is much larger for the case of single-crystal (001) Ge when compared with as-deposited amorphous Ge. Work by Impellizzeri et al.[54] compared polycrystalline versus amorphous starting material prepared by MBE and produced results similar to that of Romano et al.[28] in that the nanostructured material produced from initially polycrystalline material exhibited more elongated and larger average pore radius as compared with the nanostructured material produced from as-deposited amorphous material. Ultimately, both Romano et al.[28] and Impellizzeri et al.[54] argued that the presence of small voids within the initially amorphous material (easily observed using XTEM) were possibly serving as nucleation sites for pores during ion beam-induced structural decomposition; as the inherent voiding in the single-crystal or polycrystalline material was much less than in the case of the amorphous material, the pore density would be smaller in the former two cases as compared with the latter as there were fewer sites for pore nucleation, which was exactly what was observed experimentally. More recently, work by Yates et al.[31] systematically investigated the influence of inherent voiding in initially amorphous material by altering the deposition conditions such that voiding of the films in the as-deposited state was different. Ultimately, results consistent with those presented by Romano et al.[28] and Impellizzeri et al.[54] were produced: the density of pores was greater in the material with a greater amount of voiding in the as-deposited state and the pores were not elongated as compared with the case of single-crystal starting material.

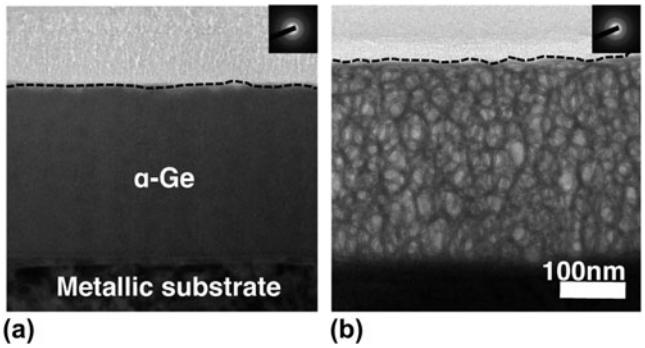


FIG. 10. XTEM images showing that ion beam modification-induced nanostructuring can also occur in initially amorphous Ge: (a) an as-deposited amorphous Ge film on a metallic substrate and (b) the same film after Ge^+-implantation at 260 keV to a dose of 1.0×10^{16} cm^{-2}. Reproduced and modified with permission from Rudawski et al.[46] Copyright © 2012 by the American Institute of Physics. Reprinted by permission of the American Institute of Physics.

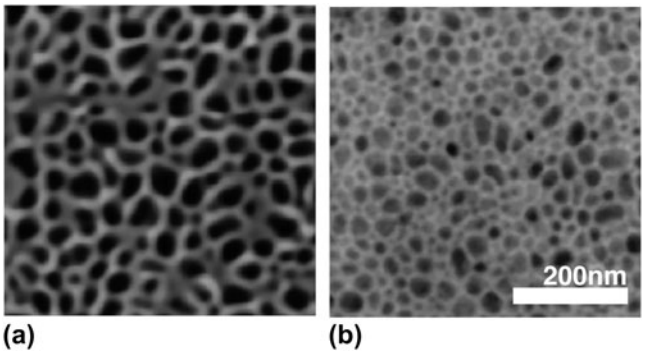


FIG. 11. Top-down SEM images of nanostructured Ge prepared via Ge^+-implantation at 300 keV to a dose of 2.0×10^{16} cm^{-2} from (a) as-deposited amorphous and (b) single-crystal (001) Ge. Reproduced and modified with permission from Romano et al.[28] Copyright © 2012 by the American Institute of Physics. Reprinted by permission of the American Institute of Physics.

https://doi.org/10.1557/jmr.2013.24 Published online by Cambridge University Press

Finally, it should be noted that some work explored the effect of "preamorphizing" a Ge single-crystal substrate and then subsequently implanting the material to induce nanostructuring.[37,55,56] However, it is unclear whether these results can be compared to the aforementioned results that used as-deposited amorphous Ge, as the cumulative effect of ion beam modification encompasses acts that both amorphize and nanostructure the material.

The results from studying generation of the nanostructured morphology using ion beam modification in initially amorphous material provide insight into the fundamental nature of the nanostructuring process. Specifically, it is evident that nucleation sites (inherent pores) appear to play an important role in the process. This observation will be returned to shortly when the different models for nanostructuring using ion beam modification are discussed.

VI. IMPLICATIONS FOR PROPOSED FORMATION MECHANISMS

To date, two different models have been advanced to explain the structural decomposition experienced by Ge as a result of ion beam modification: vacancy-clustering and microexplosions. The vacancy clustering mechanism[22,24,30,32–34] is believed to result from the inefficient recombination of point defects. In the case of pure Ge, point defect recombination is inefficient to the point that a high concentration of excess vacancies in the near-surface region of the material can result from ion beam modification as predicted by simulations. As the dose of ions is increased, the concentration of excess vacancies increases to the point at which macroscopic voids form, which is the initial stage of structural decomposition. Of course, as has already been shown, it is necessary for Ge to amorphize (or be amorphous) prior to structural decomposition. It may therefore seem counterintuitive to describe the existence of vacancies in an amorphous material. However, work strongly suggests that vacancy defects do exist in amorphous elemental semiconductors as a result of ion beam modification and that these vacancies have very similar configurations comparable to those occurring in the crystalline counterparts.[57,58] The question of the existence of vacancies in amorphous Ge due to ion beam modification notwithstanding, the main implications of the vacancy clustering model are as follows: (i) the voids should nucleate near the peak of the excess vacancies profile, (ii) the voids should nucleate in a uniform manner concomitant with the uniformity of the ion beam modification process, (iii) the total volume of voided material should increase with increasing ion dose, (iv) as vacancy motion and generation/annihilation and the crystalline to amorphous transition are thermally activated processes, nanostructuring should be sensitive to temperature during ion beam modification, and (v) the evolution of the microstructure should exhibit a ripening-like process as it would be energetically favorable for smaller pores to dissolve at the expensive of the growth of larger pores.

The microexplosion theory of nanostructuring due to ion beam modification is fundamentally different from the vacancy-clustering model.[36–39] The theory of microexplosions holds that near-surface voids are created through pressure waves caused by the overlap of ion cascades; each void is therefore the result of a microexplosion with only $\sim$0.1% of all incident ions expected to produce microexplosions. Whereas the vacancy-clustering model depends primarily on inefficiency of point defect recombination, the ability of a material to experience microexplosions during ion beam modification is dependent on ion mass/energy, bond strength, melting temperature, atomic density, and average atomic mass.[38] In terms of predictive implications that may be compared with experimental results, the microexplosion mechanism holds that (i) pores should always form near the surface regardless of incident ion energy, (ii) that the number of voids formed should always be $\sim$0.1% of the total ion dose, and (iii) the process should be independent of specimen temperature during ion beam modification as all the controlling factors are independent (or nearly independent) of temperature.

First considering the structural evolution of the nanostructured morphology with ion dose as previously described, it appears both models can explain the increase in porosity with increasing dose. However, the changes in pore morphology with ion dose as well as the observed temperature window are reasonably described only via vacancy clustering, as microexplosions are not associated with the formation, migration, and annihilation of any point defect. That being said, in the case of initially single-crystal Ge, it has been clearly and independently demonstrated that pores always nucleate at the free surface of the material and not at the peak of the expected vacancy concentration profile, which actually supports the microexplosion rather than vacancy-clustering approach. Furthermore, it was demonstrated by Darby et al.[25] in the case of initially single-crystal material that the pores tend to nucleate in clusters, rather than in a uniform manner, which is not predicted by vacancy-clustering or microexplosions mechanisms.

Of course, as shown earlier, when the material prior to ion beam modification is amorphous, the nanostructuring process evolves quite differently as compared with when the material is initially single-crystal or polycrystalline. Specifically, pores initially present in the material appear to serve as nucleation sites for further structural decomposition during ion beam modification. Additionally, the nucleation of the pores did not appear to commence at the specimen surface, but more closely near the predicted peak of the vacancy concentration profile.[31] If it is therefore assumed that some sort of nucleation site is needed for macroscopic pore formation (regardless of the nature of the starting material), a more complete picture of the mecha-

https://doi.org/10.1557/jmr.2013.24 Published online by Cambridge University Press

nism of nanostructuring due to ion beam modification can be produced.

In the case of initially single- or polycrystalline material, which is reasonably assumed to lack the inherent pores present in as-deposited amorphous Ge, amorphization followed by the generation of some sort of nucleation site are first needed. Perhaps then, a pore formed via a microexplosion in amorphized material serves as a nucleation site in this case, as first advanced by Darby et al.[25] This would explain why initial pore formation in initially crystalline material occurs only at the surface (as predicted by the microexplosions mechanism). However, the areal pore density values for a given ion dose are at least two orders of magnitude lower than predicted by the microexplosions mechanism as shown in Fig. 8 and the pores tend to nucleate in clusters rather than uniformly as shown by Darby et al.,[25] which contradicts both mechanisms. Thus, it may be in the case of initially crystalline material that a dual mechanism is responsible for nanostructuring. Specifically, a microexplosion produces a near-surface pore which serves as a nucleation point for vacancies formed during ion beam modification to cluster into additional pores; as the number of pores increases, it becomes energetically favorable for the pores to coalesce into larger pores. If the temperature of the specimen is below the temperature window for nanostructuring, vacancy clustering around the pores produced by microexplosions is suppressed. Conversely, if the temperature of the specimen is above the temperature window, the material never amorphizes and therefore cannot ever structurally decompose during ion beam modification. Of course, if the generation of microexplosions is independent of temperature, it should be possible to observe microexplosions experimentally regardless of specimen temperature during ion beam modification. However, due to the near submicroscopic nature, it is difficult in practice to experimentally observe microexplosions, especially via the use of TEM, which is critical in the characterization of the nanostructured morphology.

The consistent nucleation of the pores near the surface in initially single- or polycrystalline material is perhaps the strongest evidence in support of the microexplosions mechanism playing a role in the nanostructuring process. However, if there is any preferential diffusion of vacancies to the surface, as has been suggested to be the case in elemental semiconductors,[59] this observation may actually support the vacancy-clustering mechanism. If i.e., the case, then surface nucleation will occur as a result of the accumulation of vacancies, so it is therefore no longer necessary to invoke the use of a microexplosion to serve as a nucleation site for the generation of a pore in the case of initially single- or polycrystalline material.

In the case of initially amorphous material, there is no need for microexplosions to occur to serve as nucleation sites as inherent pores already serve as such sites, so the process should be entirely controlled by vacancy-clustering. Thus, the pores should nucleate in a uniform manner over the specimen surface and at the depth in the specimen where vacancy generation is greatest, which is consistent with observations. Also, nanostructuring should still be sensitive to the temperature window and exhibit ripening with increasing dose, which again are both consistent with experimental observations.

Thus, summarizing the experimental observations and the implications for the two proposed formation mechanisms, both may play roles depending on whether the material is initially crystalline or amorphous prior to ion beam modification. Of course, what is still not clear in either case is why the material must be amorphous prior to structural decomposition, either in the virgin state or as an intermediate state during ion beam modification.

VII. APPLICATIONS OF THE NANOSTRUCTURED MORPHOLOGY

Due to the unique morphology and relative ease of fabrication, nanostructured Ge prepared via ion beam modification has potential application in a variety of technologically relevant situations. Herein below, two of the potential applications that have shown preliminary promise are discussed: chemical sensors and energy storage.

Recent work by Impellizzeri et al.[60] studied the electrical properties of nanostructured Ge and revealed that the nanostructured morphology has unusually high electrical conductivity as compared with the crystalline and nonporous amorphous counterparts. In conjunction with the very large surface area to volume ratio, this makes the nanostructured morphology attractive for a variety of applications. In particular, it was suggested by Impellizzeri et al.[60] that the nanostructured morphology would be of potential interest in sensor applications as it was demonstrated that the material could serve as a viable template for deposition of functionalized gold (Au) nanoparticles as shown in the XTEM image presented in Fig. 12; this is significant, because it is known that the such Au nanoparticles form the basis for several different types of chemical sensors.[61]

Additionally, nanostructured Ge may have potential for use in energy storage applications. Specifically, Ge is highly attractive as a rechargeable Li ion battery (LIB) anode, as it has a theoretical specific capacity i.e., ~4.4 times that of the traditional graphite anode[62] and a very high Li^+ diffusivity.[63] However, the main challenge associated with using Ge as an LIB electrode is accommodating the large volumetric changes[62] associated with electrochemical cycling of Ge with Li; the large volumetric changes tend to cause intramaterial fracture, which leads to fading of the capacity of the electrode with prolonged electrochemical cycling.[64] In principle, this challenge can be overcome by use of the nanostructured morphology, as it has very small characteristic feature sizes, which should

https://doi.org/10.1557/jmr.2013.24 Published online by Cambridge University Press

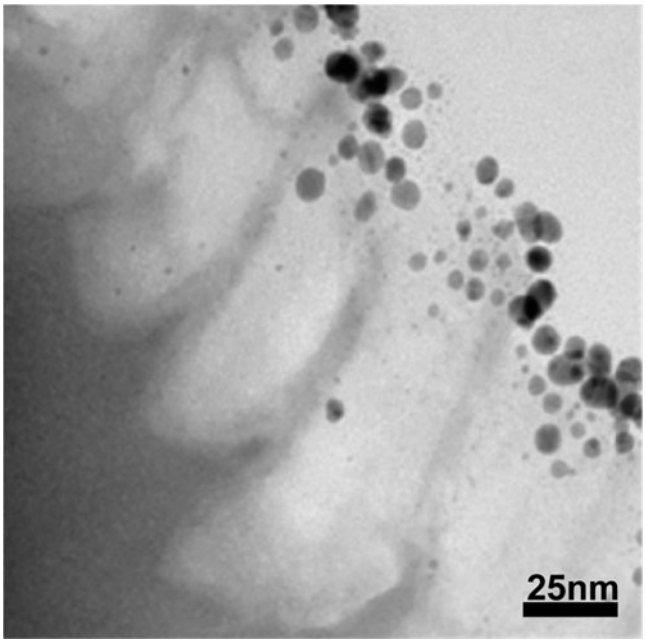


FIG. 12. XTEM image of Au nanoparticle-decorated nanostructured Ge prepared by a combination of ion beam modification (to effect nanostructuring) with subsequent electrochemical deposition (to effect Au nanoparticle decoration); this structure has potential for use in chemical sensing applications via the use of functionalized Au nanoparticles. Reproduced and modified with permission from Impellizzeri et al.[60] Copyright © 2012 by the Institute of Physics. Reprinted by permission of the Institute of Physics.

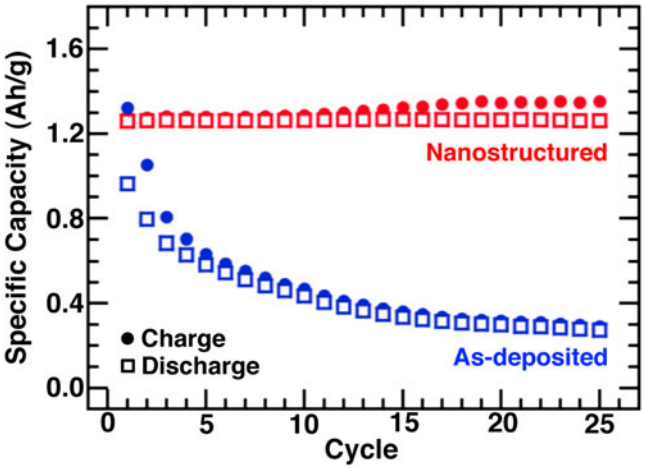


FIG. 13. Cycle life plot of a nanostructured Ge electrode prepared by electron beam deposition of amorphous Ge on a metallic substrate followed by Ge^{+}-implantation at 260 keV at room temperature to a dose of 1.0×10^{16} cm^{-2}; the electrode was electrochemically cycled with metallic Li at a C/8 rate (8 h per charge or discharge); the performance of the as-deposited version of the electrode is provided to illustrate the improvement in performance resulting from nanostructuring. Reproduced and modified with permission from Rudawski et al.[46] Copyright © 2012 by the American Institute of Physics. Reprinted by permission of the American Institute of Physics. J

be able to withstand large volumetric changes without decrepitation.[2,5] Additionally, the large surface area to volume ratio should also facilitate faster insertion and extraction of Li, which should allow for faster charging and discharging of the electrode.[2,5] In fact, the feasibility of nanostructured Ge as a LIB electrode was recently demonstrated by Rudawski et al.,[46] who showed that nanostructured Ge electrodes can withstand a large number of electrochemical cycles at a variety of cycling rate with virtually no fade in specific capacity. This is shown in Fig. 13, which presents the cycle life behavior of a nanostructured Ge electrode as compared with an as-deposited amorphous Ge electrode.

VIII. CONCLUSIONS AND FUTURE DIRECTIONS

In conclusion, the work studying nanostructuring of Ge using ion beam modification was reviewed. Specifically, the basic considerations of the morphological evolution as a function of several important variables were presented. In addition, efforts made to quantify the nanostructured morphology were also highlighted as well as the current understanding of the fundamental mechanisms governing the generation of the nanostructured morphology as well as the potential applications of nanostructured Ge with demonstrated preliminary feasibility.

Clearly, there is a relatively large amount of research that has been conducted regarding nanostructuring in Ge. However, many unanswered questions still remain. One of the most puzzling questions concerns the necessity of the material being amorphous prior to the onset of nanostructuring, as this cannot be reasonably predicted by either of the two main approaches used to explain nanostructuring. Additionally, it would be interesting to determine whether the superimposed curve for the areal pore density versus ion dose behavior indicated in Fig. 8 is consistent with observations, particularly for the relatively narrow dose range of $(2.0–5.0) \times 10^{15}$ cm^{-2} where it is expected that the pore density should actually increase with dose; verification of this predicted behavior may give further insight into whether a dual mechanism approach (microexplosions serving as nucleation sites followed by vacancy-clustering) or single mechanism approach (diffusion of vacancies to the surface with subsequent clustering) is responsible for nanostructuring in initially single- or polycrystalline material. Along these lines, the role of dose rate on morphological evolution has not been thoroughly investigated either outside of limited work where the effect on surface roughening was examined.[26] Additionally, the work reviewed in this article only reviewed cases where Ge with a free surface was ion beam-modified. Presumably, the morphological evolution of the nanostructured material may be quite different in cases where a solid-solid rather than solid-vacuum interface exists during ion beam modification. In particular, some initial work by Yates et al.[31] indicated that void nucleation does

https://doi.org/10.1557/jmr.2013.24 Published online by Cambridge University Press

not only occur at free surfaces and any inherent voids within the material, but also at solid-solid interface. A systematic study comparing nanostructuring in Ge with different solid-solid interfaces may therefore provide greater insight into the role that nucleation sites, and particularly surfaces and interfaces, play in the nanostructuring process.

A different line of investigation that may provide further insight into the fundamental aspects of nanostructuring may be the effect of alloying. Specifically, it has been shown by Romano et al.[28] that nanostructuring was avoided in deposited amorphous silicon–germanium alloy (SiGe) films with Ge content <90 at.%. However, the role of alloying in the suppression of nanostructuring is far from unclear, though it is reasonable to expect that the addition of Si to Ge would eventually suppress nanostructuring as Si does not exhibit this behavior.[65–67] Of course, it would also be interesting to see if the SiGe being initially single- or polycrystalline somehow affected this apparent "concentration window" for nanostructuring. In any case, it appears there may be some fundamental difference between Ge alloyed with Si and pure Ge i.e., influencing the nanostructuring process, which is still unclear. Extensive experimental and theoretical investigations into the role of alloying on nanostructuring using ion beam modification are therefore needed. This highlights a few of the key points for further investigation into nanostructuring of Ge using ion beam modification.

ACKNOWLEDGMENTS

The authors acknowledge Luica Romano (University of Catania, Italy) for thoughtful discussions regarding this work and for agreeing to the reproduction and modification of several figures presented in this review.

REFERENCES

1. H. Gleiter: Nanostructured materials: Basic concepts and microstructure. *Acta Mater.* **48**, 1–29 (2000).
2. A.S. Arico, P. Bruce, B. Scrosati, J.M. Tarascon, and W. Van Schalkwijk: Nanostructured materials for advanced energy conversion and storage devices. *Nat. Mater.* **4**, 366–377 (2005).
3. B. Kang and G. Ceder: Battery materials for ultrafast charging and discharging. *Nature* **458**, 190–193 (2009).
4. P. Simon and Y. Gogotsi: Materials for electrochemical capacitors. *Nat. Mater.* **7**, 845–854 (2008).
5. P.G. Bruce, B. Scrosati, and J.M. Tarascon: Nanomaterials for rechargeable lithium batteries. *Angew. Chem. Int. Ed.* **47**, 2930–2946 (2008).
6. M.S. Dresselhaus, G. Chen, M.Y. Tang, R. Yang, H. Lee, D. Wang, Z. Ren, J-P. Fleurial, and P. Gogna: New directions for low-dimensional thermoelectric materials. *Adv. Mater.* **19**, 1043–1053 (2007).
7. M. Gratzel: Mesoporous oxide junctions and nanostructured solar cells. *Curr. Opin. Colloid Interface Sci.* **4**, 314–321 (1999).
8. X-J. Huang and Y-K. Choi: Chemical sensors based on nanostructured materials. *Sens. Actuators, B* **122**, 659–671 (2007).
9. W.Y. Li, L.N. Xu, and J. Chen: Co_3O_4 nanomaterials in lithium-ion batteries and gas sensors. *Adv. Funct. Mater.* **15**, 851–857 (2005).
10. A.M. Yu, Z.J. Liang, J. Cho, and F. Caruso: Nanostructured electrochemical sensor based on dense gold nanoparticle films. *Nano Lett.* **3**, 1203–1207 (2003).
11. G. Konstantatos and E.H. Sargent: Nanostructured materials for photon detection. *Nat. Nanotech.* **5**, 391–400 (2010).
12. D.A. LaVan, T. McGuire, and R. Langer: Small-scale systems for in vivo drug delivery. *Nat. Biotech.* **21**, 1184–1191 (2003).
13. Y.M. Wang, M.W. Chen, F.H. Zhou, and E. Ma: High tensile ductility in a nanostructured metal. *Nature* **419**, 912–915 (2002).
14. J.W. Choi, J. McDonough, S. Jeong, J.S. Yoo, C.K. Chan, and Y. Cui: Stepwise nanopore evolution in one-dimensional nanostructures. *Nano Lett.* **10**, 1409–1413 (2010).
15. G.L. Destefanis and J.P. Gailliard: Very efficient void formation in ion-implanted InSb. *Appl. Phys. Lett.* **36**, 40–42 (1980).
16. D. Kleitman and H.J. Yearian: Radiation-induced expansion of semiconductors. *Phys. Rev.* **108**, 901 (1957).
17. N. Nitta, M. Taniwaki, Y. Hayashi, and T. Yoshiie: Formation of cellular defect structure on GaSb ion-implanted at low temperature. *J. Appl. Phys.* **92**, 1799–1802 (2002).
18. A. Perez-Bergquist, S. Zhu, K. Sun, X. Xiang, Y. Zhang, and L.M. Wang: Embedded nanofibers induced by high-energy ion irradiation of bulk GaSb. *Small* **4**, 1119–1124 (2008).
19. M. Shaanan, R. Kalish, and V. Richter: Changes in InSb as a result of ion implantation. *Nucl. Instrum. Methods Phys. Res., Sect. B* **7–8**, 443–447 (1985).
20. B.R. Appleton, O.W. Holland, J. Narayan, O.E. Schow, J.S. Williams, K.T. Short, and E. Lawson: Characterization of damage in ion implanted Ge. *Appl. Phys. Lett.* **41**, 711–712 (1982).
21. I.H. Wilson: The effects of self-ion bombardment (30-500 keV) on the surface topography of single-crystal germanium. *J. Appl. Phys.* **53**, 1698–1705 (1982).
22. O.W. Holland, B.R. Appleton, and J. Narayan: Ion implantation damage and annealing in germanium. *J. Appl. Phys.* **54**, 2295–2301 (1983).
23. E.M. Lawson, K.T. Short, J.S. Williams, B.R. Appleton, O.W. Holland, and O.E. Schow: Anomalous near-surface effects in room temperature implanted germanium. *Nucl. Instrum. Methods Phys. Res.* **209**, 303–307 (1983).
24. L. Romano, G. Impellizzeri, M.V. Tomasello, F. Giannazzo, C. Spinella, and M.G. Grimaldi: Nanostructuring in Ge by self-ion implantation. *J. Appl. Phys.* **107**, 084314 (2010).
25. B.L. Darby, B.R. Yates, N.G. Rudawski, K.S. Jones, A. Kontos, and R.G. Elliman: Insights for void formation in ion-implanted Ge. *Thin Solid Films* **519**, 5962–5965 (2011).
26. R.J. Kaiser, S. Koffel, P. Pichler, A.J. Bauer, B. Amon, A. Claverie, G. Benassayag, P. Scheiblin, L. Frey, and H. Ryssel: Honeycomb voids due to ion implantation in germanium. *Thin Solid Films* **518**, 2323–2325 (2010).
27. B. Stritzker, R.G. Elliman, and J. Zou: Self-ion-induced swelling of germanium. *Nucl. Instrum. Methods Phys. Res., Sect. B* **175**, 193–196 (2001).
28. L. Romano, G. Impellizzeri, L. Bosco, F. Ruffino, M. Miritello, and M.G. Grimaldi: Nanoporosity induced by ion implantation in deposited amorphous Ge thin films. *J. Appl. Phys.* **111**, 113515 (2012).
29. C.J. Glover, M.C. Ridgway, A.P. Byrne, K.M. Yu, G.J. Foran, C. Clerc, J.L. Hansen, and A.N. Larsen: Micro- and macro-structure of implantation-induced disorder in Ge. *Nucl. Instrum. Methods Phys. Res., Sect. B* **161**, 1033–1037 (2000).
30. M.C. Ridgway, C.J. Glover, K.M. Yu, G.J. Foran, C. Clerc, J.L. Hansen, and A.N. Larsen: Ion-dose-dependent microstructure in amorphous Ge. *Phys. Rev. B* **61**, 12586–12589 (2000).
31. B.R. Yates, B.L. Darby, R.G. Elliman, and K.S. Jones: Role of nucleation sites on the formation of nanoporous Ge. *Appl. Phys. Lett.* **101**, 131907 (2012).

https://doi.org/10.1557/jmr.2013.24 Published online by Cambridge University Press

32. Y.J. Chen, I.H. Wilson, W.Y. Cheung, J.B. Xu, and S.P. Wong: Ion implanted nanostructures on Ge(111) surfaces observed by atomic force microscopy. *J. Vac. Sci. Technol., B* **15**, 809–813 (1997).
33. H. Huber, W. Assmann, S.A. Karamian, A. Mucklich, W. Prusseit, E. Gazis, R. Grotzschel, M. Kokkoris, E. Kossionidis, H.D. Mieskes, and R. Vlastou: Void formation in Ge induced by high energy heavy ion irradiation. *Nucl. Instrum. Methods Phys. Res., Sect. B* **122**, 542–546 (1997).
34. L. Ottaviano, A. Verna, V. Grossi, P. Parisse, S. Piperno, M. Passacantando, G. Impellizzeri, and F. Priolo: Surface morphology of Mn^+ implanted Ge (100): A systematic investigation as a function of the implantation substrate temperature. *Surf. Sci.* **601**, 2623–2627 (2007).
35. R. Kogler, A. Mucklich, W. Skorupa, A. Peeva, A.Y. Kuznetsov, J.S. Christensen, and B.G. Svensson: Excess vacancies in high energy ion implanted SiGe. *J. Appl. Phys.* **101**, 033508 (2007).
36. P. Bellon, S.J. Chey, J.E. Vannostrand, M. Ghaly, D.G. Cahill, and R.S. Averback: Surface damage produced by 20 keV Ga bombardment of Ge (001). *Surf. Sci.* **339**, 135–141 (1995).
37. K. Gaertner, J. Joehrens, T. Steinbach, C.S. Schnohr, M.C. Ridgway, and W. Wesch: Void formation in amorphous germanium due to high electronic energy deposition. *Phys. Rev. B* **83**, 224106 (2011).
38. M. Ghaly, K. Nordlund, and R.S. Averback: Molecular dynamics investigations of surface damage produced by kiloelectronvolt self-bombardment of solids. *Philos. Mag. A* **79**, 795–820 (1999).
39. S.G. Mayr and R.S. Averback: Ion-irradiation-induced stresses and swelling in amorphous Ge thin films. *Phys. Rev. B* **71**, 134102 (2005).
40. C. Claeys, E. Simoen, K. Opsomer, D.P. Brunco, and M. Meuris: Defect engineering aspects of advanced Ge process modules. *Mater. Sci. Eng., B* **154**, 49–55 (2008).
41. A. Claverie, S. Koffel, N. Cherkashin, G. Benassayag, and P. Scheiblin: Amorphization, recrystallization and end of range defects in germanium. *Thin Solid Films* **518**, 2307–2313 (2010).
42. S. Koffel, N. Cherkashin, F. Houdellier, M.J. Hytch, G. Benassayag, P. Scheiblin, and A. Claverie: End of range defects in Ge. *J. Appl. Phys.* **105**, 126110 (2009).
43. S. Koffel, P. Scheiblin, A. Claverie, and G. Benassayag: Amorphization kinetics of germanium during ion implantation. *J. Appl. Phys.* **105**, 013528 (2009).
44. R.C. Birtcher: Energy-dependent amorphization of Ge by Ne, Ar or Kr ion irradiation. *Philos. Mag. B* **73**, 677–688 (1996).
45. N.G. Rudawski, B.R. Yates, M.R. Holzworth, K.S. Jones, R.G. Elliman, and A.A. Volinsky: Ion beam-mixed Ge electrodes for high capacity Li rechargeable batteries. *J. Power Sources* **223**, 336–340 (2013).
46. N.G. Rudawski, B.L. Darby, B.R. Yates, K.S. Jones, R.G. Elliman, and A.A. Volinsky: Nanostructured ion beam-modified Ge films for high capacity Li ion battery anodes. *Appl. Phys. Lett.* **100**, 083111 (2012).
47. J.F. Ziegler: SRIM-2003. *Nucl. Instrum. Methods Phys. Res., Sect. B* **219**, 1027–1036 (2004).
48. J.F. Prins, T.E. Derry, and J.P.F. Sellschop: Volume expansion of diamond during ion-implantation. *Phys. Rev. B* **34**, 8870–8874 (1986).
49. T. Steinbach, J. Wernecke, P. Kluth, M.C. Ridgway, and W. Wesch: Structural modifications of low-energy heavy-ion irradiated germanium. *Phys. Rev. B* **84**, 104108 (2011).
50. T. Janssens, C. Huyghebaert, D. Vanhaeren, G. Winderickx, A. Satta, M. Meuris, and W. Vandervorst: Heavy ion implantation in Ge: Dramatic radiation induced morphology in Ge. *J. Vac. Sci. Technol., B* **24**, 510–514 (2006).
51. J.C. Kim, D.G. Cahill, and R.S. Averback: Formation and annihilation of nanocavities during keV ion irradiation of Ge. *Phys. Rev. B* **68**, 094109 (2003).
52. J.C. Kim, D.G. Cahill, and R.S. Averback: Surface defects created by 20 keV Xe ion irradiation of Ge(111). *Surf. Sci.* **574**, 175–180 (2005).
53. G. Peto, Z.F. Horvath, O. Gereben, L. Pusztai, F. Hajdu, and E. Svab: Implantation-induced structural changes in evaporated amorphous Ge. *Phys. Rev. B* **50**, 539–542 (1994).
54. G. Impellizzeri, L. Romano, L. Bosco, C. Spinella, and M.G. Grimaldi: Nanoporosity induced by ion implantation in germanium thin films grown by molecular beam epitaxy. *Appl. Phys. Express* **5**, (2012).
55. T. Steinbach, C.S. Schnohr, P. Kluth, R. Giulian, L.L. Araujo, D.J. Sprouster, M.C. Ridgway, and W. Wesch: Influence of electronic energy deposition on the structural modification of swift heavy-ion-irradiated amorphous germanium layers. *Phys. Rev. B* **83**, (2011).
56. W. Wesch, C.S. Schnohr, P. Kluth, Z.S. Hussain, L.L. Araujo, R. Giulian, D.J. Sprouster, A.P. Byrne, and M.C. Ridgway: Structural modification of swift heavy ion irradiated amorphous Ge layers. *J. Phys. D* **42**, (2009).
57. S. Roorda, W.C. Sinke, J.M. Poate, D.C. Jacobson, S. Dierker, B.S. Dennis, D.J. Eaglesham, F. Spaepen, and P. Fuoss: Structural relaxation and defect annihilation in pure amorphous silicon. *Phys. Rev. B* **44**, 3702–3725 (1991).
58. G.N. Vandenhoven, Z.N. Liang, L. Niesen, and J.S. Custer: Evidence for vacancies in amorphous silicon. *Phys. Rev. Lett.* **68**, 3714–3717 (1992).
59. D.R. Lim, C.S. Rafferty, and F.P. Klemens: The role of the surface in transient enhanced diffusion. *Appl. Phys. Lett.* **67**, 2302–2304 (1995).
60. G. Impellizzeri, L. Romano, B. Fraboni, E. Scavetta, F. Ruffino, C. Bongiorno, V. Privitera, and M.G. Grimaldi: Nanoporous Ge electrode as a template for nano-sized (<5 nm) Au aggregates. *Nanotechnology* **23**, (2012).
61. H. Wohltjen and A.W. Snow: Colloidal metal-insulator-metal ensemble chemiresistor sensor. *Anal. Chem.* **70**, 2856–2859 (1998).
62. J. Sangster and A. Pelton: The Ge-Li (germanium-lithium) system. *J. Phase Equilib.* **18**, 289–294 (1997).
63. C.S. Fuller and J.C. Severiens: Mobility of impurity ions in germanium and silicon. *Phys. Rev.* **96**, 21–24 (1954).
64. R. Huggins and W. Nix: Decrepitation model for capacity loss during cycling of alloys in rechargeable electrochemical systems. *Ionics* **6**, 57–63 (2000).
65. S.M. Davidson and G.R. Booker: Damage produced by ion implantation in silicon. *Radiat. Effects* **6**, 33–43 (1970).
66. J.A. Davies, J. Denharto, L. Eriksson, and J.W. Mayer: Ion implantation of silicon. I. atom location and lattice disorder by means of 1.0-MeV helium ion scattering. *Can. J. Phys.* **45**, 4053–4071 (1967).
67. F.F. Morehead and B.L. Crowder: A model for the formation of amorphous Si by ion bombardment. *Radiat. Effects* **6**, 27–32 (1970).

https://doi.org/10.1557/jmr.2013.24 Published online by Cambridge University Press